JOURNAL OF THERMOPHYSICS AND HEAT TRANSFER
Vol. 17, No. 1, January–March 2003

Technical Notes

TECHNICAL NOTES are short manuscripts describing new developments or important results of a preliminary nature. These Notes cannot exceed six manuscript pages and three figures; a page of text may be substituted for a figure and vice versa. After informal review by the editors, they may be published within a few months of the date of receipt. Style requirements are the same as for regular contributions (see inside back cover).

Computation of Viscous Incompressible Flows with Heat Transfer Using Godunov-Projection Method

A. F. Chong* and M. Damodaran†
Nanyang Technological University, Singapore 639798, Republic of Singapore

Introduction

INCOMPRESSIBLE Navier–Stokes equations can be solved by a variety of methods such as the artificial compressibility method outlined by Chorin,[1] the pressure correction method outlined by Gresho,[2] and Chorin's[3] classical projection method. This projection method was subsequently modified to be of second order by Bell et al.[4] in which the nonlinear convective terms in the momentum equations are discretized using a specialized second-order Godunov[5] method for computing time-centered conservative differences of the nonlinear convective flux terms of the momentum equation. More recently the Godunov projection method for solving the unsteady incompressible Navier–Stokes equations and its application to a variety of incompressible flow problems have been carried out by Pan and Damodaran.[6] In this study, the Godunov-projection method for solving the momentum equations is coupled with energy equation to explore the simulation of convective flows. Cavity flows with and without forced or free heat transfer have always been popular test problems for evaluating the feasibility of various numerical schemes. The aim of the present study is to explore the possibility of computing the flow structures that develop in a lid-driven cavity subjected to a temperature gradient, by using the Godunov-projection method for solving the unsteady incompressible Navier–Stokes and energy equations. Numerous experimental and computational methods exist in the literature for the cavity flow problems, for example, Koseff and Street,[7] Prasad and Koseff,[8] and Mansour and Viskanta.[9] In this work, the simulation is demonstrated of mixed-convective heat transfer flow in a narrow, vertical cavity used by Mansour and Viskanta[9] using the Godunov-projection method[5] by introducing a temperature gradient into the flowfield to show the interaction between the shear force due to the moving lid and the buoyancy force due to the different temperatures.

Presented as Paper 2001-2971 at the AIAA 35th Thermophysics Conference, Anaheim, California, USA, 11–14 June 2001; received 13 July 2001; revision received 14 August 2002; accepted for publication 9 September 2002. Copyright © 2002 by the American Institute of Aeronautics and Astronautics, Inc. All rights reserved. Copies of this paper may be made for personal or internal use, on condition that the copier pay the $10.00 per-copy fee to the Copyright Clearance Center, Inc., 222 Rosewood Drive, Danvers, MA 01923; include the code 0887-8722/03 $10.00 in correspondence with the CCC.

*Graduate Student, Division of Thermal and Fluids Engineering, School of Mechanical and Production Engineering, Nanyang Avenue.

†Associate Professor, Division of Thermal and Fluids Engineering, School of Mechanical and Production Engineering, Nanyang Avenue. Associate Fellow AIAA.

Formulation

The nondimensional continuity, momentum, and energy equations considered are as follows:

$$\nabla \cdot \boldsymbol{U} = 0 \tag{1}$$

$$\frac{\partial \boldsymbol{U}}{\partial t} + \boldsymbol{U} \cdot \nabla \boldsymbol{U} = \frac{1}{Re}\nabla^2 \boldsymbol{U} - \nabla p + \frac{Gr}{Re^2}\boldsymbol{k}\Theta \tag{2}$$

$$\frac{\partial \Theta}{\partial t} + \boldsymbol{U} \cdot \nabla \Theta = \frac{1}{RePr}\nabla^2 \Theta + \frac{Ec}{Re}\Phi \tag{3}$$

where Φ is the temperature dissipation term associated with the nondimensional temperature, $\Theta = (T - T_c)/(T_h - T_c)$, where T is the local temperature, T_c and T_h are the cold and hot wall temperatures, respectively, $\boldsymbol{U}$ is the velocity field, p is the pressure, Re is the Reynolds number, Ec is the Eckert number, Pr is the Prandtl number, and Gr is the Grashof number. Boussinesq approximation for buoyancy-driven flows creates the last term in Eq. (2), which appears as a vertical (z direction) component along the direction in which the gravitational force is acting.

Numerical Solution Using Godunov-Projection Method

Specific details of the spatial-discretization of the convective terms of the momentum equation using the Godunov scheme that distinguishes this scheme from classical projection methods and the numerical solution of the resulting algebraic equations are described by Pan and Damodaran.[6] First, an unsplit second-order Godunov method[5] is used to compute time-centered conservative differences of the nonlinear flux terms $(\boldsymbol{U} \cdot \nabla)\boldsymbol{U}$ in Eq. (2) to provide a robust discretization scheme for overcoming the restriction of the cell Reynolds number. The Godunov method is a predictor–corrector method in which characteristics are used to extrapolate velocities to time level $t^{n+1/2}$ from the solution at time t^n. These predicted velocities are then used in a corrector step in which Riemann problems are solved to resolve ambiguities in the upwind direction, and the resultant states are used to evaluate centered difference approximations to the advective derivatives. Next, Eq. (2) is solved using a Crank–Nicholson discretization in which the pressure gradient and the nonlinear term (evaluated at the previous step) are treated as source terms. Because the pressure gradient term is lagged at time $t^{n-1/2}$, an intermediate velocity field that does not satisfy Eq. (1) is calculated. Finally, the intermediate velocity field is decomposed into divergence-free and curl-free components. The divergence-free component is the actual velocity field, whereas the curl-free component is used to update the pressure.

An economical alternative to the projection method is to create a fractional-step method that approximates the projection method to second-order accuracy that can be constructed for Eq. (2) as

$$(\boldsymbol{U}^* - \boldsymbol{U}^n)/\Delta t + \nabla p^{n-\frac{1}{2}} = (1/2Re)\nabla^2(\boldsymbol{U}^n + \boldsymbol{U}^*) - (\boldsymbol{U} \cdot \nabla \boldsymbol{U})^{n+\frac{1}{2}} + (Gr/Re^2)\boldsymbol{k}\Theta^n \tag{4}$$

where $\boldsymbol{U}^n$ is the velocity field from the previous time step and $\boldsymbol{U}^*$ is the intermediate velocity field that satisfies the same boundary condition as $\boldsymbol{U}$. The lagged pressure gradient term in Eq. (4) approximates the effect of projection. The intermediate velocity field is computed by solving Eq. (4). The decomposition of the calculated intermediate velocity field is written as

$$\boldsymbol{U}^* = \boldsymbol{U}_d + \nabla\phi \tag{5}$$

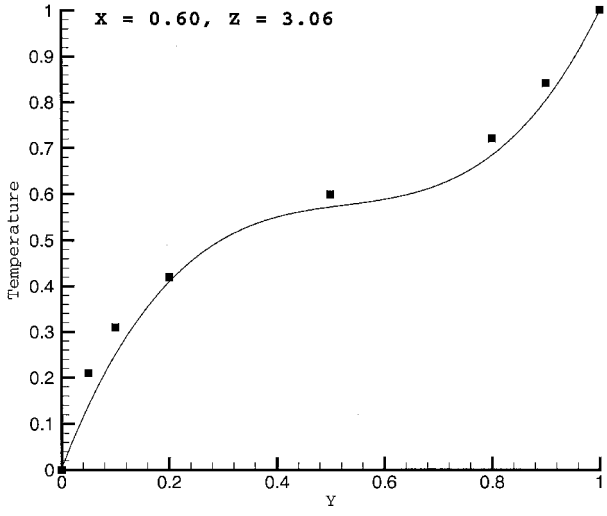

Fig. 1 Comparison of computed and experimental temperature variation at a selected location: ■, experimental values from Ref. 8 and ——, present computed results.

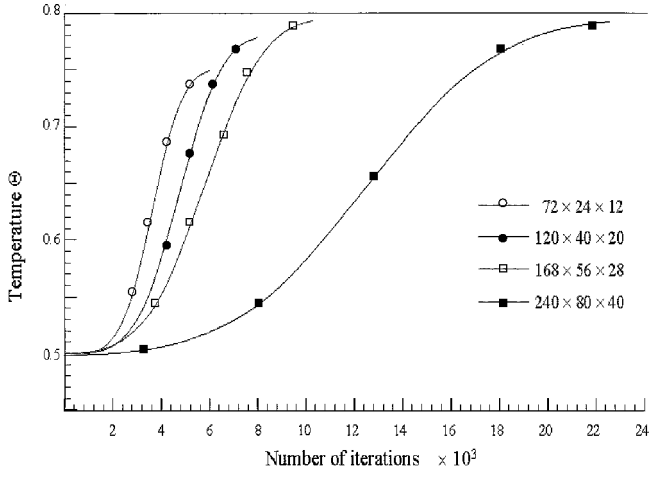

Fig. 2 Effect of grid size on the convergence of the computed solutions.

where $\boldsymbol{U}_d$ is the divergence-free velocity, or the new velocity $\boldsymbol{U}^{n+1}$, and ϕ is a scalar. A Poisson equation is formed by taking the divergence on both sides of Eq. (5),

$$\nabla^2\phi = \nabla \boldsymbol{U}^* \tag{6}$$

Equation (6) is then solved for ϕ, with the cell-centered Neumann boundary condition applied on the walls. Finally, the pressure gradient is updated by solving

$$\nabla p^{n+\frac{1}{2}} = \nabla p^{n-\frac{1}{2}} + \nabla\phi/\Delta t \tag{7}$$

Results and Discussion

The capability of the numerical scheme is demonstrated by applying it to simulate fluid and heat transfer in a lid-driven cavity whose lengths in the x–y–z directions have the ratio 6:2:1 corresponding to the experimental configuration by Mansour and Viskanta.[9] The reference velocity, which corresponds to the tangential velocity $V_0 = 0.21$ m/s imposed on the side of the cavity on the x–z plane at $y = 0$ to simulate the effect of the moving lid shearing the fluid in the cavity, is the speed of the moving lid, and the reference length L is the length of the shortest dimension of the cavity. The reference pressure P_0 is the atmospheric pressure at the room temperature of 30°C. The thermophysical properties of the fluid in the flowfield are also referenced at atmospheric pressure and room temperature and are assumed to be constant. No-slip boundary conditions are imposed on all sides of the cavity. A temperature gradient is imposed by keeping the cavity's x–z plane at $y = 0$ at a cold-wall temperature $T_c = 25$°C and the x–z plane at $y = L$ at a hot temperature $T_h = 35$°C. Adiabatic conditions are imposed on the rest of the cavity walls. The gravitational acceleration vector points in the negative z direction. The initial flow condition is assumed stagnant, and the ambient temperature is specified as the initial temperature condition. The base of the cavity lies on the x–y plane at $z = 0$.

Figure 1 shows the variation of the computed nondimensional temperature in the y direction at $z = 3.06$ on the y–z plane at $x = 0.6$. This is in good agreement with the experimental data reported at the corresponding location by Mansour and Viskanta.[9] (Mansour and Viskanta used $x = 2.94$ and $z = 1.4$ in the coordinate system.) When similar variations at various locations are compared, the maximum percentage error is about 10%, and the more significant discrepancies between the computed and experimental results appear at

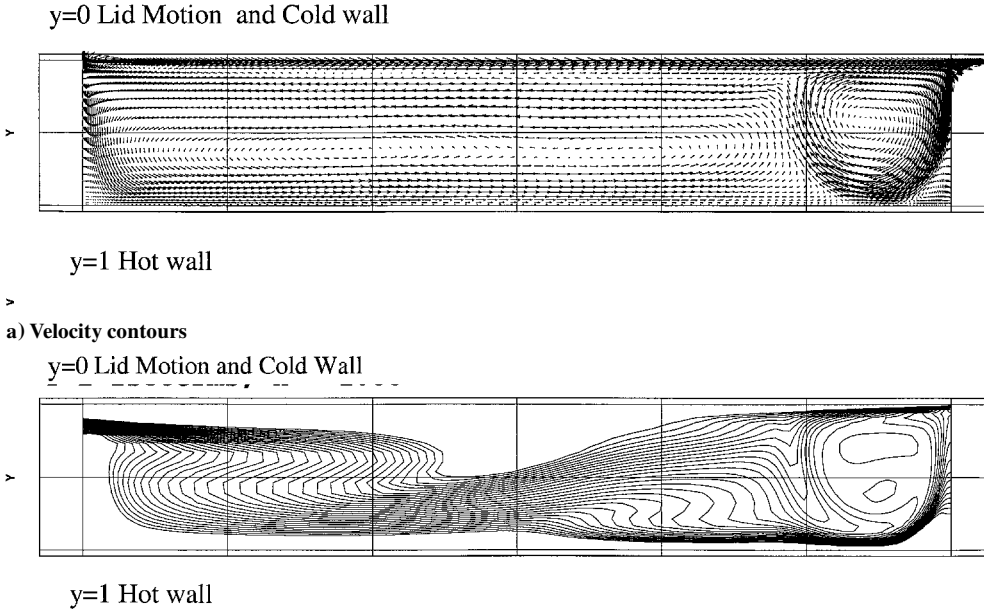

Fig. 3 Computed velocity vectors and isotherms on the y–z plane at $x = 1.0$.

locations near the bottom part of the cavity. The discrepancies could be due to the large conduction error in the temperature readings reported in the experiment. This is because the velocities in that region are small. In addition, the experiment shows that at $x = 1.0$, as the height along the z axis increases, the relative temperature correspondingly increases. This has also been observed in the computed results. The small discrepancies could be due to the assumption of the constant thermophysical properties.

The effect of grid density on the solution is shown in Fig. 2 by considering mesh sizes of $72 \times 24 \times 12$, $120 \times 40 \times 20$, and $168 \times 56 \times 28$ and by considering the converged values of the temperature at the location $(x, y, z) = (1.44, 0.80, 5.06)$. The various convergence curves begin at the initial ambient temperature of $\Theta = 0.5$, and as the grid is refined, the temperature approaches the value of 0.8, which corresponds to the experimental measurement. The $168 \times 56 \times 28$ grid gives the temperature value of approximately 0.79, with a 1.25% error. Further increase in the grid size beyond this size does not improve the value significantly.

Figure 3a shows the computed velocity vector field, and Fig. 3b shows the corresponding temperature contours on the middle y–z plane at $x = 1.00$, from which a recirculating fluid flow near the top of the cavity and a small secondary vortex just above the recirculating flow can be seen. This is caused by the entrapment of the pocket of fluid in the corner. As a temperature gradient is introduced into the flow, buoyancy effects will cause the flow of the fluid to be directed upward in the positive z direction. This buoyancy effect can be seen clearly in the vicinity of the hot wall, where the temperature T_h is imposed. It can be seen that the flowfield is divided into two distinct regions, the downward flow on the cooler side of the cavity and the upward flow on the hotter side. At about $y = 0.4$, it can be seen that the flow is virtually stagnant. The flow that is moving downward is driven mainly by inertia, whereas the flow that is moving upward is driven completely by buoyancy. The numerical results compare well with the flowfield contours based on the experimental data and the method has captured the relevant thermofluid physics of convective flows very well. Detailed results of the simulation can be found in Chong and Damodaran.[10]

Conclusions

In this study, the Godunov-projection method has been used to solve for the viscous incompressible flow with heat transfer in a lid-driven cavity. This projection method circumvents the problem arising from the lack of the time dependency of the density in the continuity equation. The energy equation is included with the momentum equations to solve the temperature field. The comparison between the numerical results and the experimental data shows good agreement thereby demonstrating the feasibility of using this algorithm for fluid flows with heat transfer. The maximum percentage error is about 10% and is mostly due to the large conduction error at the bottom of the cavity. The numerical simulation of the cavity flow reveals clearly the viscous effects at the wall boundaries and the shear force at the moving lid boundary. Grid convergence studies indicate that a grid size of $168 \times 56 \times 28$ and above is required to obtain numerical results that are within 1.25% of the experimental results. The present study has only focused on the feasibility of the numerical scheme to study steady-state convective flows. Future work will address the more general unsteady cavity flow in which perturbations will be imposed on the boundary conditions to simulate unsteady thermal and flow effects and the steady-state solutions obtained here will be used as the initial conditions to capture the evolving unsteady flowfields. The assumption of constant fluid properties will be discarded, and the governing equations will be modified to take into account the temperature dependency by way of coupling.

References

[1]Chorin, A. J., "A Numerical Method for Solving Incompressible Viscous Flow Problems," *Journal of Computational Physics*, Vol. 2, 1967, pp. 12–26.

[2]Gresho, P. M., "Some Current CFD Issues Relevant to the Incompressible Navier–Stokes Equations," *Computer Methods in Applied Mechanics and Engineering*, Vol. 87, 1991, pp. 201–252.

[3]Chorin, A. J., "Numerical Solution of the Navier–Stokes Equations," *Mathematics of Computations*, Vol. 22, Oct. 1968, pp. 745–762.

[4]Bell, J. B., Colella, P. and Howell, L. H., "An Efficient Second-Order Projection Method for Viscous Incompressible Flow," *Proceedings of the 10th AIAA Computational Fluid Dynamics Conference*, AIAA, Washington, DC, 1991, pp. 360–367.

[5]Godunov, S. K., "A Difference Scheme for Numerical Computation of Discontinuous Solution of Hydrodynamic Equations," *Math. Sbornik.*, Vol. 47, 1959, pp. 271–306.

[6]Pan, H., and Damodaran, M., "Parallel Computation of Viscous Incompressible Flows Using Godunov-Projection Method on Overlapping Grids," *International Journal of Numerical Methods in Fluids*, Vol. 39, No. 5, 2002, pp. 441–463.

[7]Koseff, J. R., and Street, R. L., "On End Wall Effects in a Lid-Driven Cavity Flow," *Journal Fluids Engineering*, Vol. 106, Dec. 1984, pp. 385–389.

[8]Prasad, A. K., and Koseff, J. R., "Combined Forced and Natural Convection Heat Transfer in a Deep Lid-Driven Cavity Flow," *International Journal of Heat and Fluid Flow*, Vol. 17, No. 5, 1996, pp. 460–467.

[9]Mansour, R. B., and Viskanta, R., "Shear-Opposed Mixed-Convection Flow and Heat Transfer in a Narrow, Vertical Cavity," *International Journal of Heat and Fluid Flow*, Vol. 15, No. 6, 1994, pp. 462–469.

[10]Chong, A. F., and Damodaran, M., "Parallel Computation of Viscous Incompressible Flows with Heat Transfer Using Second-Order Projection Methods," AIAA Paper 2001-2971, June 2001.

Buoyancy Effects on Three-Dimensional Convection Flow Adjacent to Backward-Facing Step

J. H. Nie* and B. F. Armaly†
University of Missouri–Rolla, Rolla, Missouri 65409

Introduction

SEPARATED and reattached flow occurs in many heat-exchanging devices, such as electronic and power generating equipment and dump combustors. A great deal of mixing of high- and low-energy fluid occurs in the separated and reattached flow regions, thus impacting significantly the heat transfer performance of these devices. Studies on separated flow have been conducted extensively during the past decades, and the backward-facing step geometry has received most of the attention.[1–3] The majority of published work dealt with the two-dimensional flow, and comparatively little is published about the three-dimensional nonisothermal case. Such knowledge is critical for optimizing the performance of physical heat-exchanging devices because they have mostly three-dimensional and nonisothermal flow. Forced convection results have been reported for a duct with an aspect ratio of 12 by Pepper and Carrington[4] and with an aspect ratio of 8 by Armaly et al.[5] To the authors' knowledge, the work of Iwai et al.[6] on the effects of duct inclination angle on heat transfer for a duct with aspect ratio of 16 and the work of Li and Armaly[7,8] on mixed convection in a duct with an aspect ratio of 8 are the only published three-dimensional results that incorporate the buoyancy force in the analysis for this simple geometry.

Received 1 September 2001; revision received 4 August 2002; accepted for publication 13 August 2002. Copyright © 2002 by the American Institute of Aeronautics and Astronautics, Inc. All rights reserved. Copies of this paper may be made for personal or internal use, on condition that the copier pay the $10.00 per-copy fee to the Copyright Clearance Center, Inc., 222 Rosewood Drive, Danvers, MA 01923; include the code 0887-8722/03 $10.00 in correspondence with the CCC.

*Postdoctoral Fellow, Department of Mechanical and Aerospace Engineering and Engineering Mechanics.

†Curators' Professor, Department of Mechanical and Aerospace Engineering and Engineering Mechanics.